International Journal of Technology 15(3) 481-491 (2024)
Received September 2021/ Revised January 2022 / Accepted August 2023

International Journal of Technology

Robust Sliding Mode Controller Design for Boost Converter Applications

Hussain Attia[1*], Freddy Tan Kheng Suan[2]

[1]*Department of Electrical & Electronics Engineering, American University of Ras Al Khaimah, Ras Al Khaimah, 72603, United Arab Emirates*
[2]*Department of Electrical and Electronic Engineering, University of Nottingham Malaysia, Jalan Broga, 43500 Semenyih, Selangor*

Abstract. This paper presents detailed steps to design an effective, robust sliding mode controller for boost converter applications. Before that, the paper models a boost converter circuit during a continuous conduction mode (CCM) operation, obtains the related dynamic equations and explains the variation effects of the circuit parameters on the converter performance. The design steps of the proposed controller are illustrated, and the robustness of the controller is demonstrated in terms of maintaining output voltage stability under input voltage variations and load fluctuations. On the other hand, this paper shows a fast and accurate dynamic response of the load voltage during different reference voltages. Simulation results are collected, analyzed, and demonstrated the robustness and correctness of the proposed controller design.

Keywords: Boost converter; Converter modeling; Simulation; Sliding mode control

1. Introduction

Due to the advancement of technology in the field of renewable energy sources, DC-DC converters largely penetrated in implementing the power electronic systems to generate clean electricity (Andreas *et al.*, 2018; Setiawan and Setiawan, 2017; Shafinaz *et al.*, 2016; Rini *et al.*, 2014). On the other side, support for renewable energy sources is exemplified by microgrids, which combine various renewable energy sources and can be interconnected with the electrical grid (Rahul, 2023; Budiyanto *et al.*, 2011). DC-DC converter plays a major role in the standalone and/or grid-connected power electronic systems by converting a variable DC link voltage to a desired output-regulated DC voltage. The converter is stepping up the input voltage using a DC-DC boost converter, stepping down the input voltage using a DC-DC buck converter, or able to step up/step down the input voltage using a DC-DC buck/boost converter (Shayeghi, Poujafar, and Sedaghati, 2020; Ali, Hossein, and Amir, 2014; Sulistiyanto, Rif'an, and Setyawati, 2014).

All converter circuits involve capacitors, inductors, transistors, and diodes for energy storing and directing from the source side to the load side (Deepak *et al.*, 2018; Walker and Sernia, 2004) showed an integrated comparison among converter types and highlighted the functions of the converter parameters. Based on the converter parameters, the converter can operate in either continuous conduction mode CCM, in which the minimum inductor current will be more than zero amperes, or the converter can operate in discontinuous conduction mode DCM, in which the minimum inductor current can be zero amperes during

*Corresponding author's email: hattia@aurak.ac.ae, Tel.: +971 7 246 8888, Fax.: +971 7 246 8888
doi: 10.14716/ijtech.v15i3.5164

a certain frequently switching period (Emerson *et al*., 2021; Philippe and Peter, 2020; Saravana *et al.* 2014).

By considering the design difficulty of the DC-DC boost converter, the successful controlling scheme should manipulate the variation in the input voltage, the desired reference voltage, and the variation of the connected load, in addition to the possibility of connected nonlinear loads. So, a robust and accurate controller such as Sliding Mode Controller SMC is necessary to have an effective converter performance (Makhloufi, Bousserhane, and Zegnoun, 2021; Sattianadan *et al.*, 2020).

At the same time, it deserves to be mentioned that many research studies proposed a successful design to suppress the chattering demerit in the controlling input voltage to the SM controller (Huayang *et al*., 2023; Xin, Huashan, and Wenke, 2021; Mobayen *et al.*, 2021; Amirzubir *et al.,* 2016).

This paper models a DC-DC boost converter and demonstrates a detailed sliding mode controller design suitable for controlling the boost converter. The study started by modeling the converter, obtaining the dynamic equations, explaining the design steps of the desired SMC, and then evaluating the converter performance by analyzing the collected Simulink simulation results. The remainder of this paper is as follows: modeling a DC-DC boost converter and driving the related dynamic equations shown in Section 2, detailed design steps and equations of a sliding mode controller explained in Section 3. Simulating the proposed SMC with a DC-DC boost converter and collecting and analyzing the collected simulation results are all demonstrated in Section 4. Section 5 summarizes the conclusion of this study.

2. Modelling of DC-DC Boost Converter

A boost converter or a step-up converter works on having a regulated output load voltage of a level greater than the input voltage level. This converter has been implemented by adding an LC low-pass filter to a basic converter circuit (Farzin, 2021; Attia, 2020a; 2020b; Daniel and Hart, 2011; Rashid, 2001). Figure 1 shows the circuit of the DC-DC boost converter. In this converter, the diode will be reverse-biased when the switch is ON, whereas the diode is directing the inductor current during the OFF state of the switch.

Figure 2(a) shows the equivalent converter circuit when the switch is ON and the diode is reverse biased, whereas Figure 2 (b) shows the equivalent converter circuit when the switch is OFF and the diode is forward biased.

When the switch is ON (close), the source voltage across the inductor is shown in Equation 1, whereas Equation 2 demonstrates the inductor current derivative.

$$v_L = V_s = L\frac{di}{dt} \tag{1}$$

$$\frac{di}{dt} = \frac{V_s}{L} \tag{2}$$

The behavior of the current derivative is linear and positive during the switch closing, Equation 3 demonstrates this current derivative during this period. Equation 4 shows the variation in inductor current with respect to the duty ratio D.

$$\frac{di}{dt} = \frac{\Delta i}{\Delta t} = \frac{\Delta i_L}{DT} = \frac{V_s}{L} \tag{3}$$

$$(\Delta i_L)_{close} = \frac{V_s\, DT}{L} \tag{4}$$

When the switch is open, the diode becomes forward-biased to provide a path for inductor current, which cannot change instantaneously. By assuming constant output voltage (V_o), the voltage across the inductor is shown in Equation 5, and based on that the inductor current during opening the switch is demonstrated by Equation 6.

$$v_L = V_s - V_o = L\frac{di}{dt} \quad (5)$$

$$\frac{di_L}{dt} = \frac{V_s - V_o}{L} \quad (6)$$

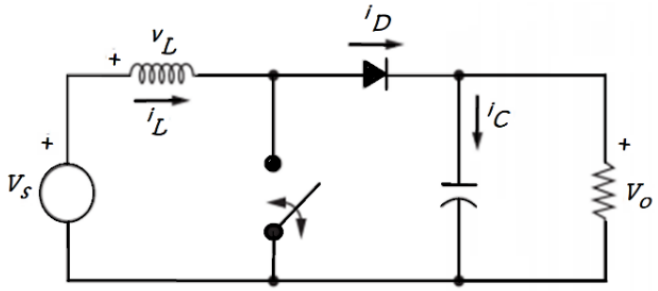

Figure 1 DC-DC boost converter circuit

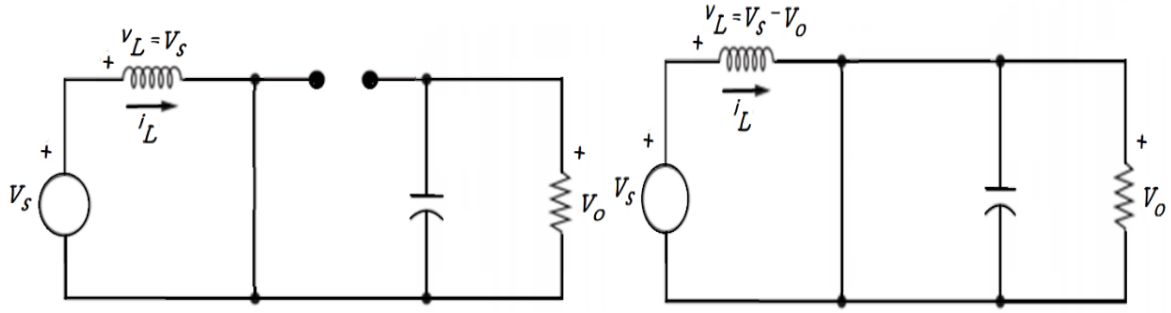

(a) (b)

Figure 2 DC-DC boost converter; (a) Converter circuit when the switch is ON, (b) Converter circuit when the switch is OFF

Equation 7 shows the inductor current derivative during the switch OFF (open), whereas Equation 8 shows the inductor current change with respect to duty ratio *D*.

$$\frac{di_L}{dt} = \frac{\Delta i}{\Delta t} = \frac{\Delta i_L}{(1-D)T} = \frac{V_s - V_o}{L} \quad (7)$$

$$(\Delta i_L)_{open} = \frac{(V_s - V_o)(1-D)\,T}{L} \quad (8)$$

During steady-state operation, the net change in inductor current for each one switching period is zero as demonstrated Equation 9, and it can demonstrated after variables replacement as shown in Equation 10. Based on that Equation 11 shows the converter output voltage.

$$(\Delta i_L)_{close} + (\Delta i_L)_{open} = 0 \quad (9)$$

$$\frac{V_s\,DT}{L} + \frac{(V_s - V_o)(1-D)\,T}{L} = 0 \quad (10)$$

Or,

$$V_o = \frac{V_s}{1-D} \quad (11)$$

From Equation 11, the boost converter produces an output voltage that is greater than or equal to the input voltage based on the instantaneous value of the Duty cycle (*D*).

The instantaneous value of the inductor current variation Δi_L or $\frac{di_L}{dt}$ equal to the summation of $\Delta i_{L\,Close}$ and $\Delta i_{L\,Open}$. By considering the duty cycle (*DT)* is (*u)* for the switch ON time, (*T-DT)* is (*1-u)* for the switch OFF time, the dynamic equation of $\frac{di_L}{dt}$ can be written as shown in Equation 12, and can be rearrange as shown in Equation 13.

$$\frac{di_L}{dt} = (\Delta i_L)_{close} + (\Delta i_L)_{open} \quad (12)$$

$$\frac{di_L}{dt} = \frac{V_s}{L} - (1 - u)\frac{V_o}{L} \quad (13)$$

When the switch is OFF (open), the inductor current equals to the summation of the capacitor and the resistor current as shown in Equation 14. Based on that Equation 15 demonstrates the capacitor current, and it can be written by considering the capacitor voltage derivative multiplying by the capacitance value as shown in Equation 16. Equation 17 shows the expression of the capacitor derivative by moving the capacitance to the right side.

$$(1 - u)i_L = i_C + i_R \quad (14)$$

$$i_C = (1 - u)i_L - \frac{V_o}{R} \quad (15)$$

$$C\frac{dV_o}{dt} = (1 - u)i_L - \frac{V_o}{R} \quad (16)$$

Or,

$$\frac{dV_o}{dt} = \frac{(1-u)}{C}i_L - \frac{V_o}{RC} \quad (17)$$

Equations (13) and (17) represent the dynamic equations of the inductor current and output voltage of the DC-DC boost converter, respectively.

3. Design of Sliding Mode Controller

The function of the Sliding Mode (SM) controller is to decide the switching state u of the converter switch (Tahri, Tahri, and Flazi, 2014; Saad *et al.*, 2011; Guldemir, 2011; Guldemir, 2005; Trushev *et al.*, 2005). The sliding surface S of the boost converter can be represented by the summation of error in the output voltage as shown in Equation 18, which is the difference between the reference voltage and actual output voltage ($x_1 = V_{ref} - V_o$), and x_2, which is the change of the error of the output voltage dx_1/dt as demonstrated in Equation 19.

$$S(x) = x_1 + x_2 \quad (18)$$

$$S(x) = x_1 + \frac{dx_1}{dt} \quad (19)$$

Replace x_1 by (V_{ref} -V_o), and $\frac{dx_1}{dt}$ by$(-\frac{dV_o}{dt})$ in Equation 19 yields sliding surface in circuit parameters form as shown in Equation 20, and Equation 21.

$$S(x) = \left(V_{ref} - V_o\right) - \frac{1}{C}\left(i_L - \frac{V_o}{R}\right) \quad (20)$$

Or,

$$S(x) = -\frac{1}{C}i_L + \left(\frac{1-RC}{RC}\right)V_o + V_{ref} \quad (21)$$

Sliding mode control depends on the objective of the slide mode S, and the derivative of the surface $\dot{S}$ to be zero value as indicated in Equation 22.

$$S(x) = \dot{S}(x) = 0 \quad (22)$$

So $\dot{S}$ can be determined by doing derivative to the surface S as shown in Equation 23.

$$\dot{S} = -\frac{1}{C}\frac{di_L}{dt} + \frac{1-RC}{RC}\frac{dV_o}{dt} \quad (23)$$

Replacing Equation 13 and Equation 17 in Equation 23 yields Equation 24 which demonstrates the derivative of S.

$$\dot{S} = -\frac{1}{C}\left(\frac{V_s}{L} - (1 - u)\frac{V_o}{L}\right) + \left(\frac{1-RC}{RC}\right)\left(\frac{(1-u)}{C}i_L - \frac{V_o}{RC}\right) \quad (24)$$

The general structure of the controlling state u includes two components as shown in Equation 25: equivalent controlling component u_{eq}, and the nonlinear component u_n (Tahri, Tahri, and Flazi, 2014; Saad *et al.*, 2011; Guldemir, 2011);

$$u = u_{eq} + u_n \quad (25)$$

Equaling $\dot{S}$ to zero yields the equivalent control of switching ON state u_{eq} as demonstrated in Equation 26.

$$u_{eq} = \frac{Ai_L + BV_o - FV_s}{FV_o + Ai_L} \quad (26)$$

where the equivalent values of the parameters A, B, and F are demonstrated in Equation 27, Equation 28, and Equation 29 respectively.

$$A = \frac{1-RC}{RC^2} \quad (27)$$

$$B = \frac{R^2C + LRC - L}{LR^2C^2} \quad (28)$$

$$F = \frac{1}{LC} \quad (29)$$

The nonlinear component u_n can be defined as shown in Equation 30.

$$u_n = sign\ (S) \quad (30)$$

Figure 3 demonstrates the DC-DC boost converter circuit controlled by the designed sliding mode controller through the Pulse Width Modulation PWM technique to generate the drive pulses.

4. Simulation with Results Analysis

Simulation of the boost converter is done using MATLAB®/Simulink® version 2015b after selecting a fixed switching frequency of 15 kHz. Many practical research studies have been focused on using a low switching frequency starting from 1.2 kHz in power converter applications to have an effective power electronic system with low switching losses (Busacca *et al.* 2022; Rohten *et al.* 2021; Ye, Malysz, and Emadi, 2015; Abrishamifar, Ahmad, and Mohamadian, 2012). Table 1 shows the simulated converter parameters, which were selected by considering the work of (Abouchabana *et al.*, 2021; Attia, 2020a; Attia, 2020b). Table 1 also demonstrates the range of simulated input voltage, reference voltage, connected load, and converter parameters, which are determined through the relationships of (Sreedhar and Basavaraju, 2018).

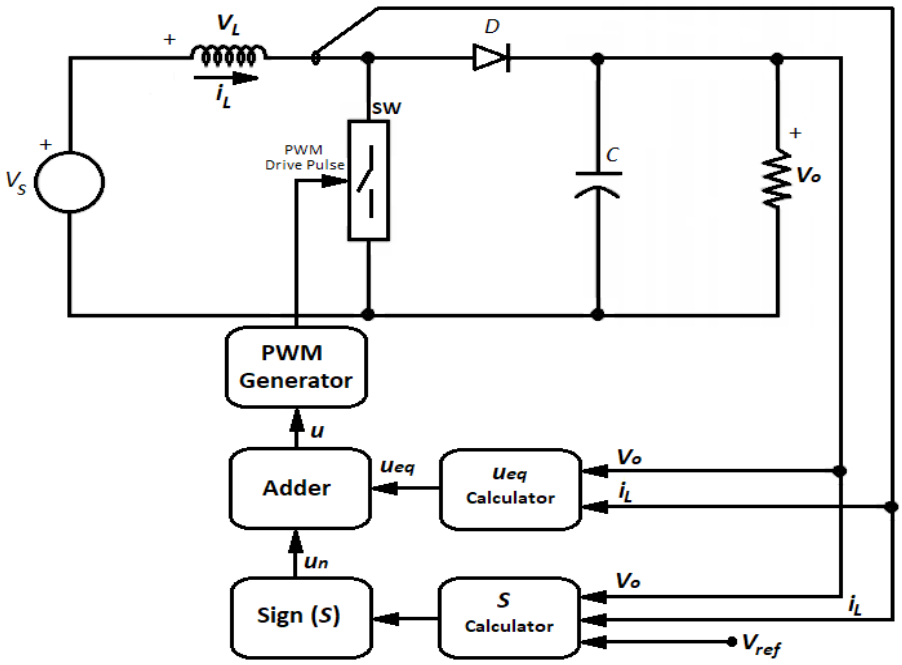

Figure 3 Block diagram of the proposed Sliding Mode Controller SMC for DC-DC boost converter

Table 1 Parameters for testing the SMC-based converter

Converter Parameter	Parameters Value
Inductor	5 mH
Capacitor	2200 µF
Connected load	12 Ω, 24 Ω
Input voltage for (Vo = 30 V)	15 V, 20 V, 24 V
Reference voltage for (Vs = 20 V)	30 V, 35 V, 40 V
Switch frequency f_s	15 kHz
Sampling time	5×10^{-7} sec or 0.5 µsec

Figure 4 shows the MATLAB/Simulink simulation of the proposed converter controlled by the designed sliding mode controller, whereas Figure 4(b) shows the details of the calculated SMC parameters.

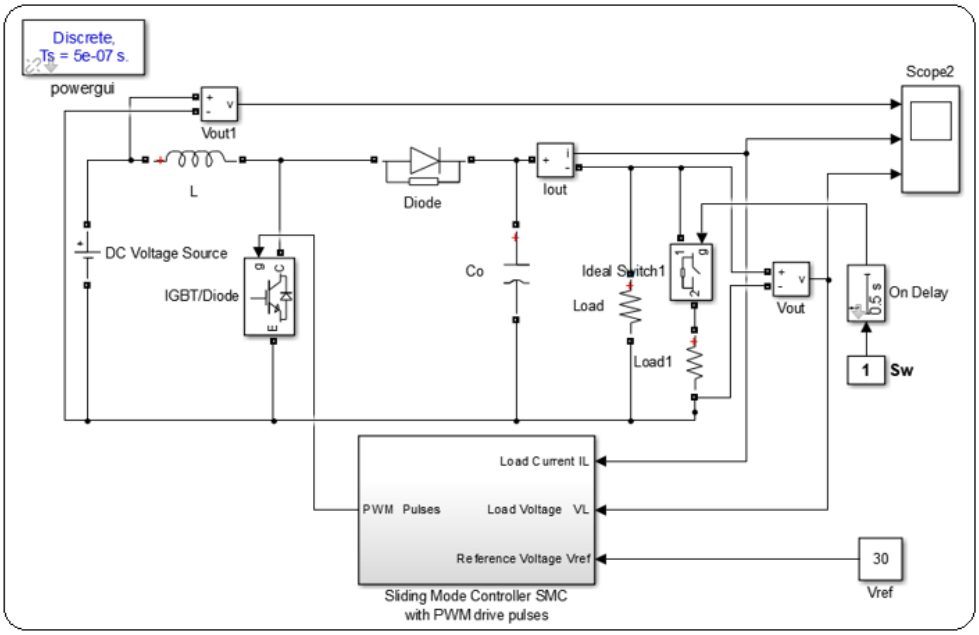

(a)

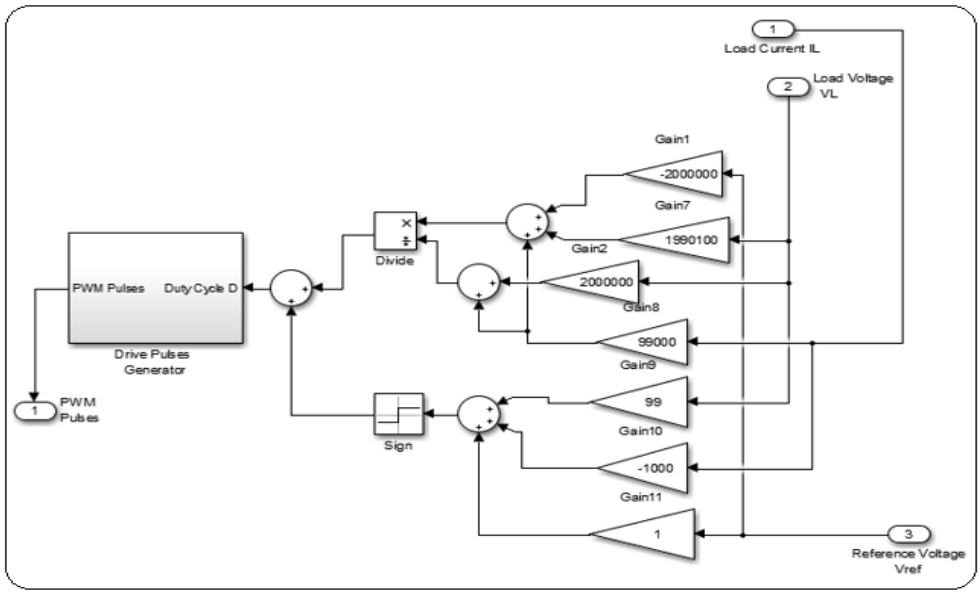

(b)

Figure 4 MATLAB/Simulink simulation of proposed system, (a) The SM controller with DC-DC boost converter, (b) Simulation of the designed SM controller with the calculated parameters

Figure 5 illustrates the robustness and accuracy of the controller under a fixed source voltage of 20 Volts, focusing on load voltage regulation. The load voltage is maintained at 30 V while the load varies from 24 Ω for the initial 0.5 seconds of simulation to 12 Ω for the subsequent 0.5 seconds, covering the entire simulation time of 1 second. Figure 5(b) shows a zoom-in of the starting transient response, in which the increments in load current and load voltage are clearly noticeable at each step of sampling time 0.5 µsec with soft starting without any overshoot in the load voltage and load current. Figure 5(c) shows a zoom-in view of the system response during a steady period, in which measuring a short period approximately equals 67 µsec (14.9 kHz), whereas measuring a long period approximately equals 133 µsec (7.5 kHz). Figure 5(d) shows a zoom-in view of the system response during the same steady period, in which measuring a long period approximately equals 133 µsec (7.5 kHz). In other words, the sliding mode controller controls the switching frequency of the PWM drive pulses based on the status of the sliding surface and, consequently, the instantaneous level of the duty cycle.

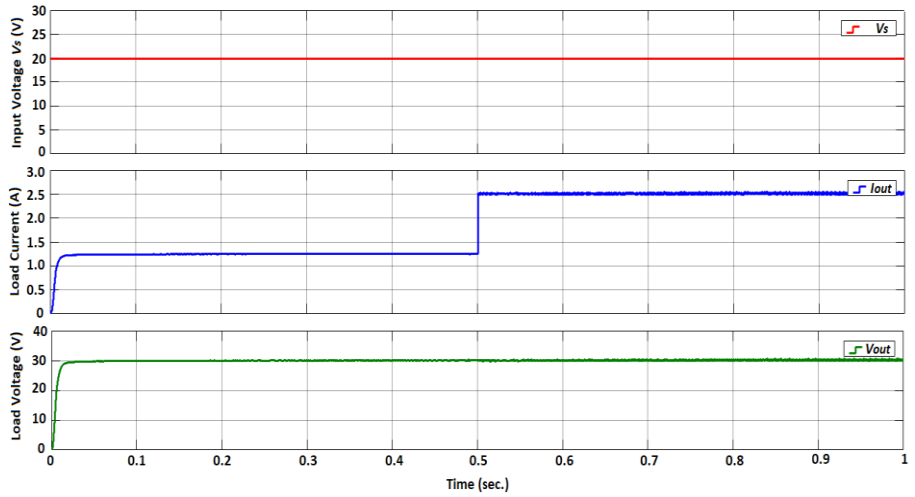

(a)

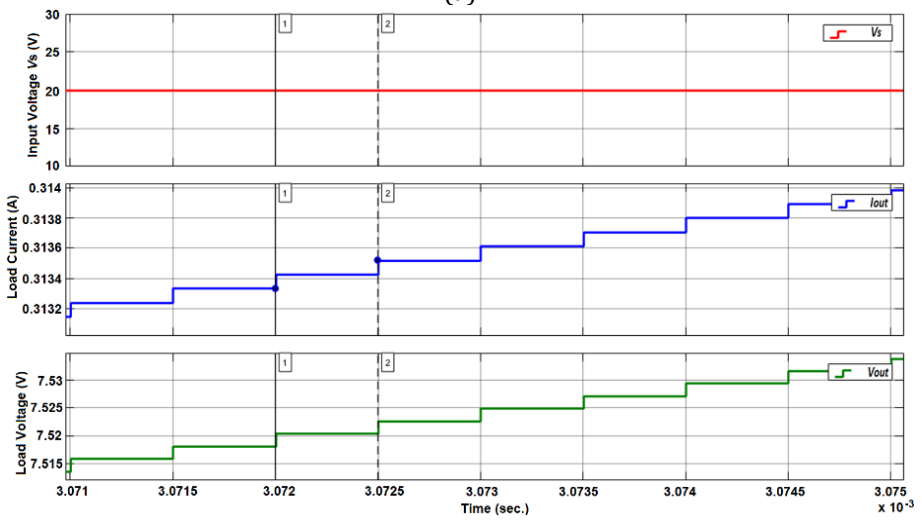

(b)

Figure 5 Load voltage and current when load resistor 24 Ω, then 12 Ω, (a) Results of 1 sec simulation period, (b) Zoom in during the transient period, (c) Zoom in during steady period with time measuring of the high switching frequency range, (d) Zoom in during steady period with time measuring of the low switching frequency

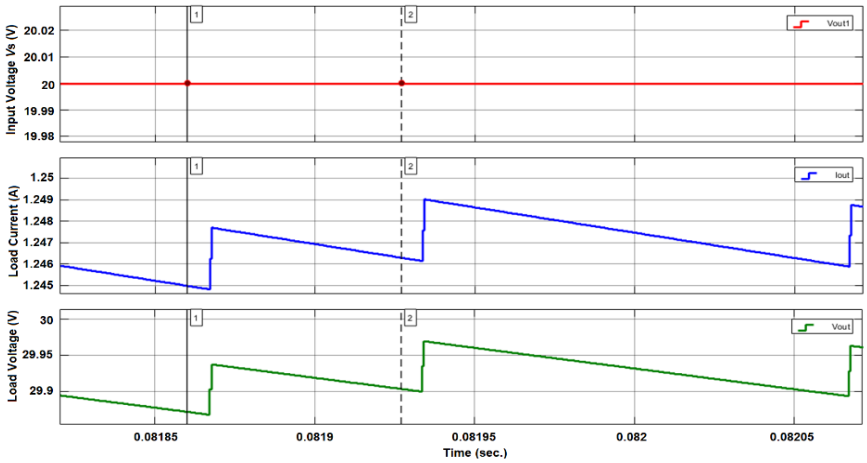

(c)

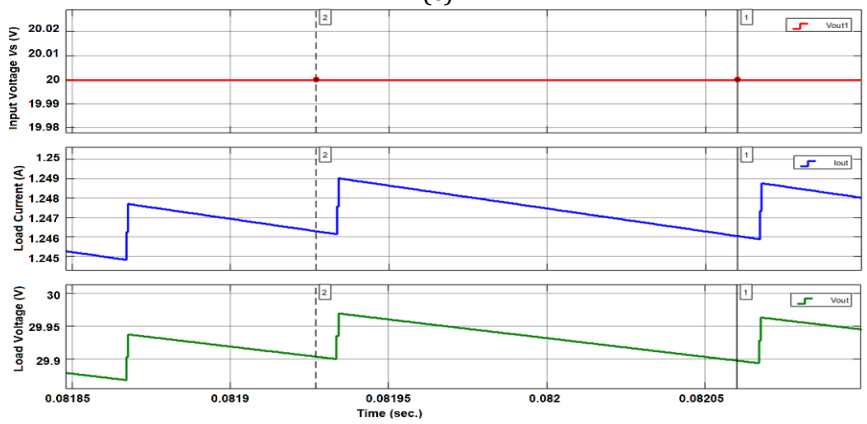

(d)

Figure 5 Load voltage and current when load resistor 24 Ω, then 12 Ω, (a) Results of 1 sec simulation period, (b) Zoom in during the transient period, (c) Zoom in during steady period with time measuring of the high switching frequency range, (d) Zoom in during steady period with time measuring of the low switching frequency (Cont.)

Figure 6 illustrates the controller response at various reference voltages. The simulation initiates with a reference voltage of 30 Volts for the first quarter of the 1-second simulation period. Subsequently, reference voltages of 35 Volts, 40 Volts, and 35 Volts are applied for the remaining three-quarters of the simulation period. As depicted in Figure 6, the load voltage accurately tracks the reference voltage. Figure 7 demonstrates the controller's effectiveness and response during the variation of input source voltage.

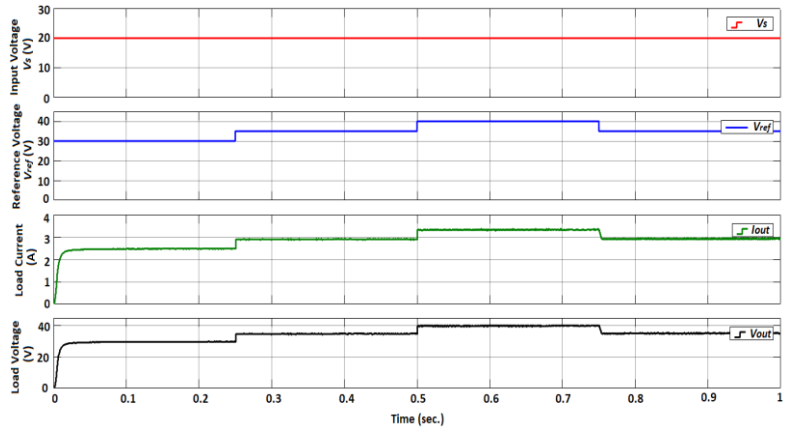

Figure 6 Load voltage and current at different V_{ref} (30 V, 35 V, 40 V, 35 V) when load resistor 12 Ω

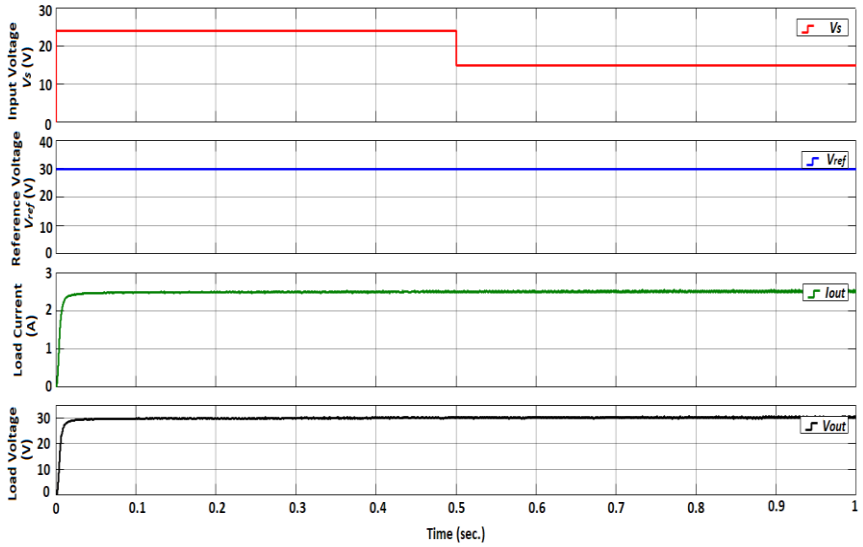

Figure 7 Load voltage and current at different Vs (24 V, 15 V) when load resistor 12 Ω

5. Conclusions

The paper has presented a comprehensive demonstration of the detailed steps involved in designing a sliding mode controller for DC-DC boost converters. Initially, the paper covered the modeling of the converter circuit during continuous conduction mode (CCM) operation. Subsequently, the paper outlines the design steps of a robust SM controller to decide the instantaneous value of the controlling state involving the effects of equivalent controlling components and nonlinear components. Simulation results have been collected and analyzed using MATLAB/Simulink software. The study's findings and analysis underscore the effectiveness and robustness of the designed controller, particularly in coping with variations in source voltage and connected loads. Furthermore, it is demonstrated that the controller adeptly tracks the instantaneous reference voltage.

Acknowledgments

The author expresses gratitude for the financial support received from the Office of Research & Community Service at the American University of Ras Al Khaimah, UAE, https://aurak.ac.ae/en/academics/office-of-research-community-service/.

References

Abouchabana, N., Haddadi, M., Rabhi, A., Grasso, A.D., Tina, G.M., 2021. Power Efficiency Improvement of a Boost Converter Using a Coupled Inductor with a Fuzzy Logic Controller: Application to a Photovoltaic System. *Applications of Machine Learning for Renewable Energy based Modern Power Systems,* Volume 11, 980, pp. 1–19

Abrishamifar, A., Ahmad, A., Mohamadian, M., 2012. Fixed Switching Frequency Sliding Mode Control for Single-Phase Unipolar Inverters. *IEEE Transactions on Power Electronics*, Volume 27(5), pp. 2507–2514

Ali, A., Hossein, A., Amir, Fz., 2014. Design, Analysis and Implementation of a Buck–Boost DC/DC Converter. *IET Power Electron*., Volume 7(12), pp. 2902–2913

Amirzubir, S., Farzin, P., Mohammad, H.M., Reza, A., Hootan, G., Nasri, B.S., 2016. Methodologies of Chattering Attenuation in Sliding Mode Controller. *International Journal of Hybrid Information Technology.* Volume 9(2), pp. 11–36

Andreas, J., Setiawan, E.A., Halim, S., Atar, M., Shabrina, H.N., 2018. Performance Test of 2.5 KW DC Boost Converter for Nanogrid System Applications*. International Journal of Technology*, Volume 6, pp. 1285–1294

Attia, H., 2020. A New Intelligent Power Factor Corrector for Converter Applications. *In*: 9th International Conference on Advanced Information Technologies and Applications (ICAITA 2020), pp. 189–199

Attia, H., 2020. Artificial Neural Network Based Unity Power Factor Corrector for Single Phase DC-DC Converters. *International Journal of Electrical and Computer Engineering*, Volume 10(4), pp. 4145–4154

Budiyanto, Setiabudy, R., Setiawan, E.A., Sudibyo, U.B., 2011. Development of Direct Current Microgrid Control for Ensuring Power Supply from Renewable Energy Sources. *International Journal of Technology,* Volume 2(3), pp. 199–206

Busacca, A., Di Tommaso, A.O., Miceli, R., Nevoloso, C., Schettino, G., Scaglione, G., Volia, F., Colak, I., 2022. Switching Frequency Effects on The Efficiency and Harmonic Distortion in A Three-Phase Five-Level CHBMI prototype with multicarrier PWM schemes: Experimental analysis. *Energies,* Volume 15, p. 586

Daniel, W., Hart, 2011. *Power Electronics*. New York, USA: McGraw-Hill

Deepak, R., Bandi, M.R., Shimi, S.L., Paulson, S., 2018. Bidirectional dc to dc Converters: An verview of Various Topologies, Switching Schemes and Control Techniques. *International Journal of Engineering & Technology*, 7 (4.5), pp. 360–365

Emerson, M., Duberney, M., Carlos, R., Javier, M., Roberto, G., 2021. Modelling of SEPIC, Cuk and Zeta Converters in ´Discontinuous Conduction Mode and Performance Evaluation. *Sensors*, Volume 21(7434), pp. 1–28

Farzin, A., 2021. On the Dynamical Modelling of DC-DC Converters. *Balkan Journal of Electrical & Computer Engineering*, Volume 9(4), pp. 371–378

Guldemir, H., 2005. Sliding Mode Control of Dc-Dc Boost Converter. *Journal of Applied Sciences*, Volume 5(3), pp. 588–592

Guldemir, H., 2011. Modeling and Sliding Mode Control of Dc-Dc Buck-Boost Converter. *In*: 6th International Advanced Technologies Symposium (IATS'11), pp. 475–480

Huayang, S., Zhang, E., Chunyang, H., Zhenbang, X., 2023. Chattering-free Fast Fixed-time Sliding Mode Control for Uncertain Robotic Manipulators*. International Journal of Control Automation and Systems,* Volume 21(2), pp. 630–644

Makhloufi, K., Bousserhane, I.K., Zegnoun, S.A., 2021. Adaptive Fuzzy Sliding Mode Controller Design for PMLSM Position Control. *International Journal of Power Electronics and Drive Systems*, Volume 12(2), pp. 674–684

Mobayen, S., Bayat, F., Lai, C. C., Taheri, A., Fekih, A., 2021. Adaptive Global Sliding Mode Controller Design for Perturbed DC-DC Buck Converters. *Energies*, Volume 14(5), p. 1249

Philippe, G., Peter, W.L., 2022. Discontinuous Conduction Mode Operation of the Current Shaping Modular Multilevel Dc-DC Converter. *IEEE Journal of Emerging and Selected Topics in Power Electronics*. Volume 10(2), pp. 2233–2244

Rahul, K.J., 2023. Sustainable Energy Transition: Analyzing the Impact of Renewable Energy Sources on Global Power Generation. *Journal of Artificial Intelligence and Capsule Networks.* Volume 5(3), pp. 314–330

Rashid, M.H., 2001. *Power electronics*. Handbook. New York, USA: Academic Press

Rini, N.H., Frediawan, Y., Onny, S., Hadi, S., Dian, R.S., Taufik, T., 2014. A Modified Perturb-and-Observe Control for Improved Maximum Power Point Tracking Performance on Grid-Connected Photovoltaic System. *International Journal of Technology,* Volume 15(1), pp. 99–109

Rohten, J.A., Muñoz, J.E., Pulido, E.S., Silva, J.J., Villarroel, F.A., Espinoza, J.R., 2021. Very Low Sampling Frequency Model Predictive Control for Power Converters in The Medium and High-Power Range Applications. *Energies,* Volume 14(1), p. 199

Saad, K.B., Sahbani A., Benrejeb, M., Bartoszewicz, A., 2011. Sliding Mode Control and Fuzzy Sliding Mode Control for DC-DC Converters. In: *Sliding Mode Control*, pp. 1–24

Saravana, D., Mohammed, J., Umayal, V., Indumathi, M., 2014. Simulation of Fuzzy Logic Control Based MPPT Technique for Photovoltaic System. *In*: 2nd International Conference on Innovations in Engineering and Technology (ICCET'2014), pp. 10–14

Sattianadan, D., Kumar, G.P., Sridhar, R., Reddy, K.V., Reddy, B.S.U., Mamatha, P., 2020. Investigation of low voltage DC microgrid using sliding mode Control. *International Journal of Power Electronics and Drive Systems*, Volume 11(4), pp. 2030–2037

Setiawan, A., Setiawan, E.A., 2017. Optimization of a Photovoltaic Power Plant in Indonesia with Proper Tilt Angle and Photovoltaic Type using a System Advisor Model. *International Journal of Technology,* Volume 8(3), pp. 539–548

Shafinaz, A.L., Hossain, S., Hasan, M.K., Chak, T.K., 2016. Design and Simulation of DC-DC Converters. *International Research Journal of Engineering and Technology (IRJET),* Volume 3(1), pp. 63–70

Shayeghi, H., Poujafar, S., Sedaghati, F., 2021. A Buck-Boost Converter; Design, Analysis and Implementation Suggested for Renewable Energy Systems. *Iranian Journal of Electrical and Electronic Engineering*, Volume 17(2), pp. 1–14

Sreedhar, J., Basavaraju, B., 2018. Plan and Analysis of Synchronous Buck Converter for UPS Application. *International Journal of Engineering & Technology*, Volume 7 (1), pp. 679–684

Sulistiyanto, N., Rif'an, M., Setyawati, O., 2014. Development of a 20V-LED Driver based on the Boost Converter using a FPGA Module. *International Journal of Technology,* Volume 5(3), pp. 287–292

Tahri, F., Tahri, A., Flazi, S., 2014. Sliding Mode Control for DC-DC Buck Converter. *In*: 3rd International Conference on Power Electronics and Electrical Drives (ICPEED'14), Volume 14, pp. 1–5

Trushev, I., Mastorakis, N., Tabahnev, I., Mladenov, V., 2005. Adaptive Sliding Mode Control For DC/DC Buck Converters. *WSEAS Transactions on Electronics,* Volume 2(4), pp. 109–113

Walker, G.R., Sernia P.C., 2004. Cascaded Dc-Dc Converter Connection of Photovoltaic Modules. *IEEE Transactions on Power Electronics,* Volume 19, pp. 1130–1139

Xin, C., Huashan, L., Wenke, L., 2021. Chattering-Suppressed Sliding Mode Control for Flexible-Joint Robot Manipulators. *Actuators*, Volume 10(288), pp. 1–24

Ye, J., Malysz, P., Emadi, A., 2015. A Fixed-Switching-Frequency Integral Sliding Mode Current Controller for Switched Reluctance Motor Drives. *IEEE Journal of Emerging and Selected Topics in Power Electronics,* Volume 3(2), pp. 381–394